ABDOMINAL IMAGING

Iran J Radiol. 2018 October; 15(4):e65346. doi: 10.5812/iranjradiol.65346.

Published online 2018 July 3. **Case Report**

Synchronous Occurrence of Classic and Scirrhous Hepatocellular Carcinomas: A Case Report

Seung Soo Kim [1,*], Jeong Ah Hwang [1], Hyeong Cheol Shin [1], Soon Auck Hong [2], Sung Shick Jou [1], Woong Hee Lee [1], Chan Ho Park [1] and Seo-Youn Choi [3]

[1]Department of Radiology, Cheonan Hospital, Soonchunhyang University College of Medicine, Cheonan-si, Korea
[2]Department of Pathology, Cheonan Hospital, Soonchunhyang University College of Medicine, Cheonan-si, Korea
[3]Department of Radiology, Bucheon Hospital, Soonchunhyang University College of Medicine, Bucheon, Korea

[*]*Corresponding author*: Seung Soo Kim, Department of Radiology, Cheonan Hospital, Soonchunhyang University College of Medicine, 31 Soonchunhyang6-gil, Dongnam-gu, Cheonan-si, Chungcheongnam-do, 330-721, Republic of Korea. Tel: +82-415703515, Fax: +82-415703516, E-mail: radiology2008@hanmail.net

Received 2017 December 20; **Revised** 2018 April 10; **Accepted** 2018 April 17.

Abstract

Scirrhous hepatocellular carcinoma (HCC) is a subtype of HCC that is characterized by abundant fibrous stroma admixed with tumor cells. Although imaging findings of scirrhous HCC differ from those of classic HCC, it is difficult to diagnose this rare neoplasm. Like classic HCC, scirrhous HCC frequently develops in patients with liver cirrhosis, but there has been no report of synchronous occurrence of classic and scirrhous HCCs. Here, we report synchronous classic and scirrhous HCCs in a 62-year-old man with early liver cirrhosis who underwent gadoxetic acid-enhanced and diffusion-weighted magnetic resonance imaging.

Keywords: Hepatocellular carcinoma, Neoplasms, Multiple Primary, 'Scirrhous' type, MRI

1. Introduction

Hepatocellular carcinoma (HCC) is the most common primary liver cancer and one of the leading causes of death worldwide (1). HCC is categorized as classic, fibrolamellar, spindle cell variant, clear cell, pleomorphic, and scirrhous HCC (2). Among these various subtypes, scirrhous HCC is a rare tumor that shows intense fibrous stroma (3). Several studies investigating imaging findings of scirrhous HCC reported that scirrhous HCC showed different imaging features from classic HCC in both computed tomography (CT) and magnetic resonance (MR) imaging (4-7). However, because of its rarity and similar imaging features to those of other liver cancers with fibrosis, it is difficult to diagnose scirrhous HCC using imaging tools (8). Scirrhous HCC similar to classic HCC is associated with liver cirrhosis. However, to the best of our knowledge, synchronous occurrence of scirrhous and classic HCCs has not been reported (3).

Here, we report a case of synchronous classic and scirrhous HCCs in a 62-year-old man who underwent gadoxetic acid-enhanced and diffusion-weighted (DW) MR imaging.

2. Case Presentation

A 62-year-old man was admitted to our hospital in October 2016 for further evaluation of a hepatic mass that was incidentally detected at a local clinic. He had a history of alcohol consumption greater than 80 g/day for longer than 30 years. The patient was negative for hepatitis B surface antigen (HBsAg) and anti-hepatitis C virus (HCV) antibody. Abnormal laboratory results were as follows: aspartate aminotransferase (AST), 45 IU/mL (normal, $\leq$ 40); γ-glutamyltransferase (γ-GTP), 129 IU/mL (normal, 6 - 60 IU/mL); α-fetoprotein, 14.43 ng/mL (normal, < 8); and protein induced by vitamin K absence-II, 6,923 mAU/mL (normal, $\leq$ 40). Other laboratory studies were in the normal range: white blood cell count, 7,280/mm^3; hemoglobin, 13.2 g/dL; hematocrit, 39.5%; platelet count, 211,000/mm^3; alanine aminotransferase (ALT), 33 IU/mL; total protein, 7.7 g/dL; albumin, 4.6 g/dL; calcium, 9.5 mg/dL; phosphorus, 3.2 mg/dL; prothrombin time (PT), 10.3 seconds; international normalized ratio (INR), 0.95; and activated partial thromboplastin time (aPTT), 27.4 seconds.

Portal venous phase images on abdominal CT obtained at an outside hospital showed two abutting hepatic masses in segments 8 and 7 (Figure 1). The mass in segment 8 had a thin capsule and a size of 6.6 $\times$ 6.2 cm, while a 6.2 $\times$ 5.5 cm sized mass in segment 7 showed a thick enhancing rim.

The patient underwent gadoxetic acid-enhanced and DW MR imaging for detailed evaluation of the hepatic masses. The masses were hypointense and hyperintense on fat suppressed T1- and T2-weighted images, respectively

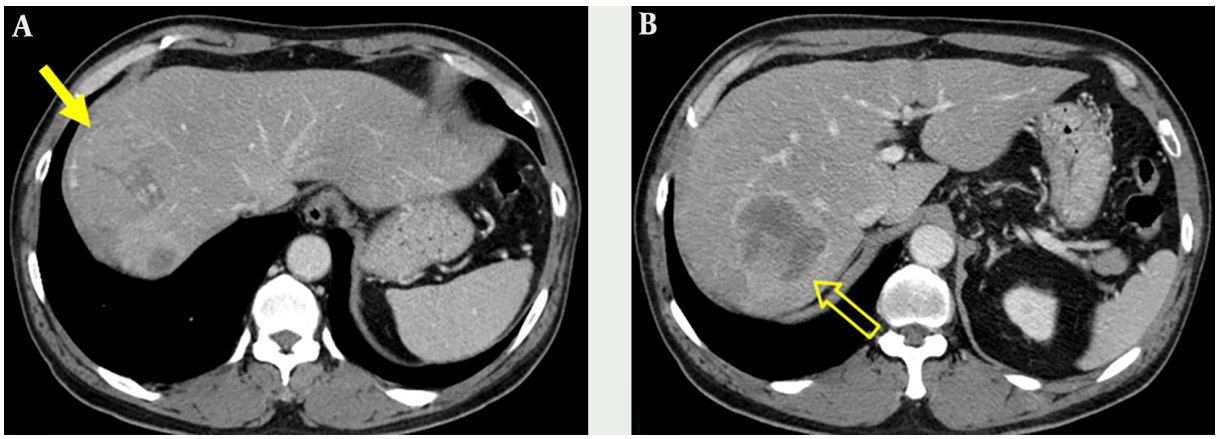

Figure 1. A 62-year-old man with an incidentally detected hepatic mass. Contrast-enhanced portal venous phase CT images obtained at an outside hospital. Axial contrast-enhanced CT image shows a 6.6-cm isoattenuating mass (arrow) with capsular enhancement in segment 8 of the liver (A) and another 6.2-cm sized mass (open arrow) with irregular and thick enhancing rim in segment 7(B).

(Figures 2A, 2B, 3A, and 3B). On DW image, the mass in segment 8 showed diffusion restriction as a whole, while the mass in segment 7 revealed diffusion restriction in the periphery (Figures 2C, 2D, 3C, and 3D). In the dynamic contrast-enhanced images, the mass in segment 8 had proper radiologic findings for diagnosis of HCC, including arterial hyperenhancement with delayed washout and capsule, and showed hypointensity on hepatobiliary phase (HBP) image (Figure 2E - 2G). In contrast, the mass in segment 7 showed hypervascularity of the periphery on arterial phase followed by centripetal enhancement, and a target appearance on HBP image (Figure 3E - 3H). We suspected that the tumor in segment 7 was an intrahepatic cholangiocarcinoma (IHCC) and ordered percutaneous liver biopsy. Ultrasonography (USG)-guided percutaneous liver biopsies were performed with two different devices to avoid pathologic contamination. The hepatic masses showed hypo-echogenicity on USG (Figure 4). Histologic examination of the biopsy specimen documented that the mass in segment 8 was HCC (Edmonson-Steiner grade II) and the second mass in segment 7 was a poorly differentiated carcinoma. After 1 month, the patient underwent right hemihepatectomy under a diagnosis of synchronous HCC and IHCC.

The resected liver demonstrated two hepatic masses, one measured 6.7 × 6 cm in segment 8 and another of 6 × 5.5 cm in segment 7. The tumor in segment 8 was characterized by a well-defined nodule with light brown coloration and hemorrhagic foci, whereas the tumor in segment 7 had a lobulated contour with whitish cut surface and showed dense fibrosis (Figure 5A). There was no evidence of satellite nodules and lymph node metastasis. On histologic examination, the two hepatic masses were closely abutted but were separated by non-neoplastic liver (Figure 5B). In the tumor in segment 8, polygonal tumor cells with eosinophilic cytoplasm were arranged in a trabecular and pseudoglandular pattern (Figure 5C). The tumor in segment 7 was composed of polygonal cells and characterized by abundant and diffusely distributed fibrous stroma (Figure 5D). Tumor cells in both segment 8 and 7 were negative for cytokeratin 19 (Figure 5E). Mucin production was not identified by mucicarmine staining. Thus, the masses in segment 8 and 7 were diagnosed as classic HCC and scirrhous HCC, respectively. In non-neoplastic liver, complete and bridging fibrosis were demonstrated. Moderate fatty change with no significant portal and lobular inflammation was found (Figure 5F). The histologic findings were consistent with early cirrhosis associated with alcohol consumption. He has been followed up on CT every 3 to 6 months, and there was no recurrence until 16 months after surgery.

Ethical approval: all procedures in studies involving human participants were performed in accordance with the ethical standards of the institutional and/or national research committee and with the 1964 Helsinki declaration and its later amendments or comparable ethical standards. This article does not contain any studies with animals performed by any of the authors. Formal consent is not required for this type of study.

3. Discussion

Scirrhous HCC is a rare hepatic neoplasm that was first described by Omata et al. (9). Although the precise incidence of scirrhous HCC in the general population is not available due to its low prevalence, a previous study reported that 4.6% (25/546) of consecutively resected HCCs

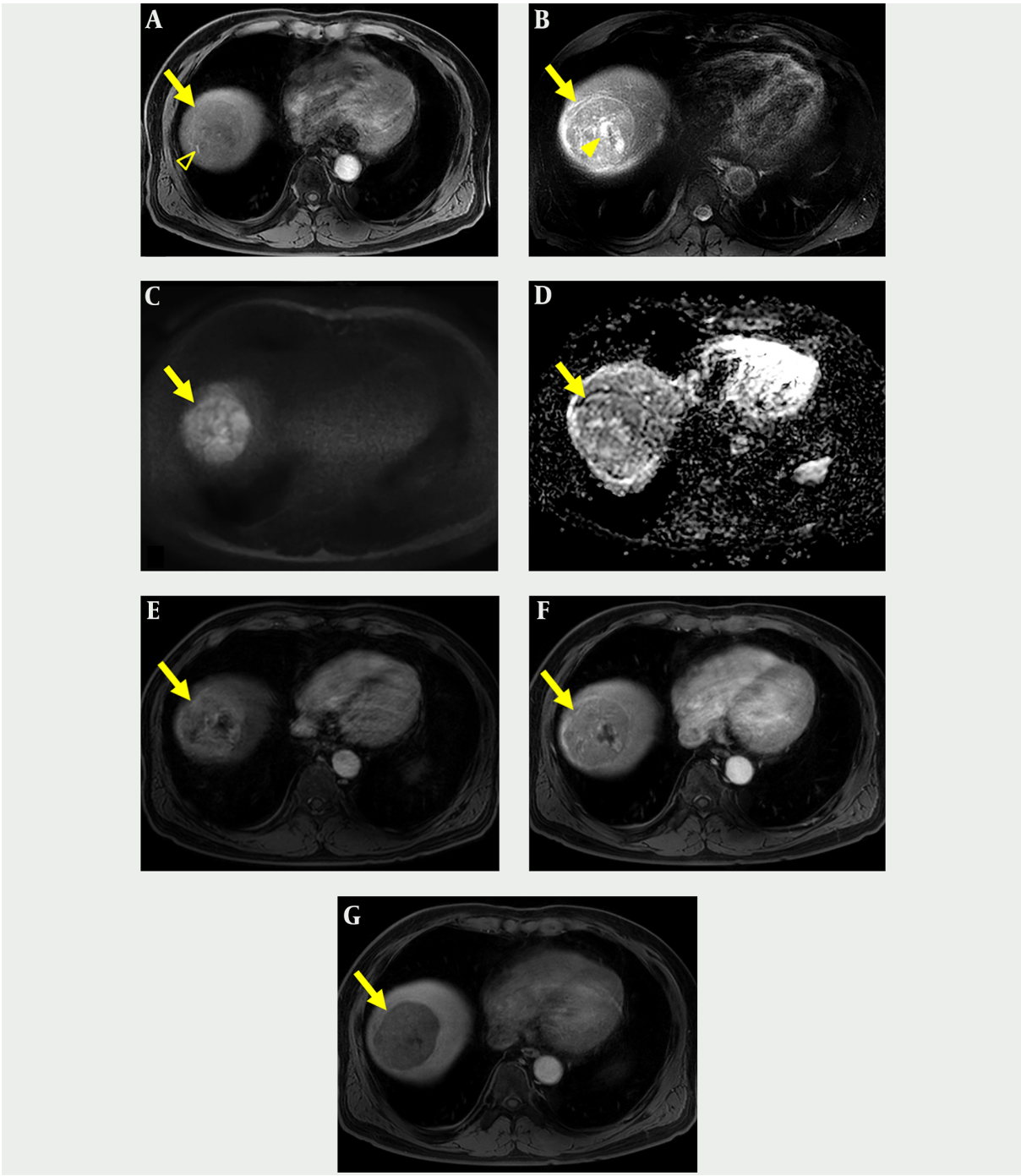

Figure 2. Gadoxetic acid-enhanced and diffusion-weighted MR imaging of classic hepatocellular carcinoma (HCC). A, Axial T1-weighted image shows a hypointense mass (arrow) with well-demarcated margin in segment 8 that contains hyperintense foci indicating hemorrhage (open arrowhead); B, Axial T2-weighted image shows a hyperintense mass (arrow) with cystic or necrotic portion (arrowhead); C and D, Axial diffusion weighted image (b = 800 s/mm^2) and apparent diffusion coefficient map show the mass (arrow) with diffusion restriction. E and F, Axial contrast-enhanced arterial and portal venous phase images show arterial hyperenhancement with delayed washout and capsular enhancement of the mass (arrow); G, Axial hepatobiliary phase image shows a mass (arrow) with hypointensity.

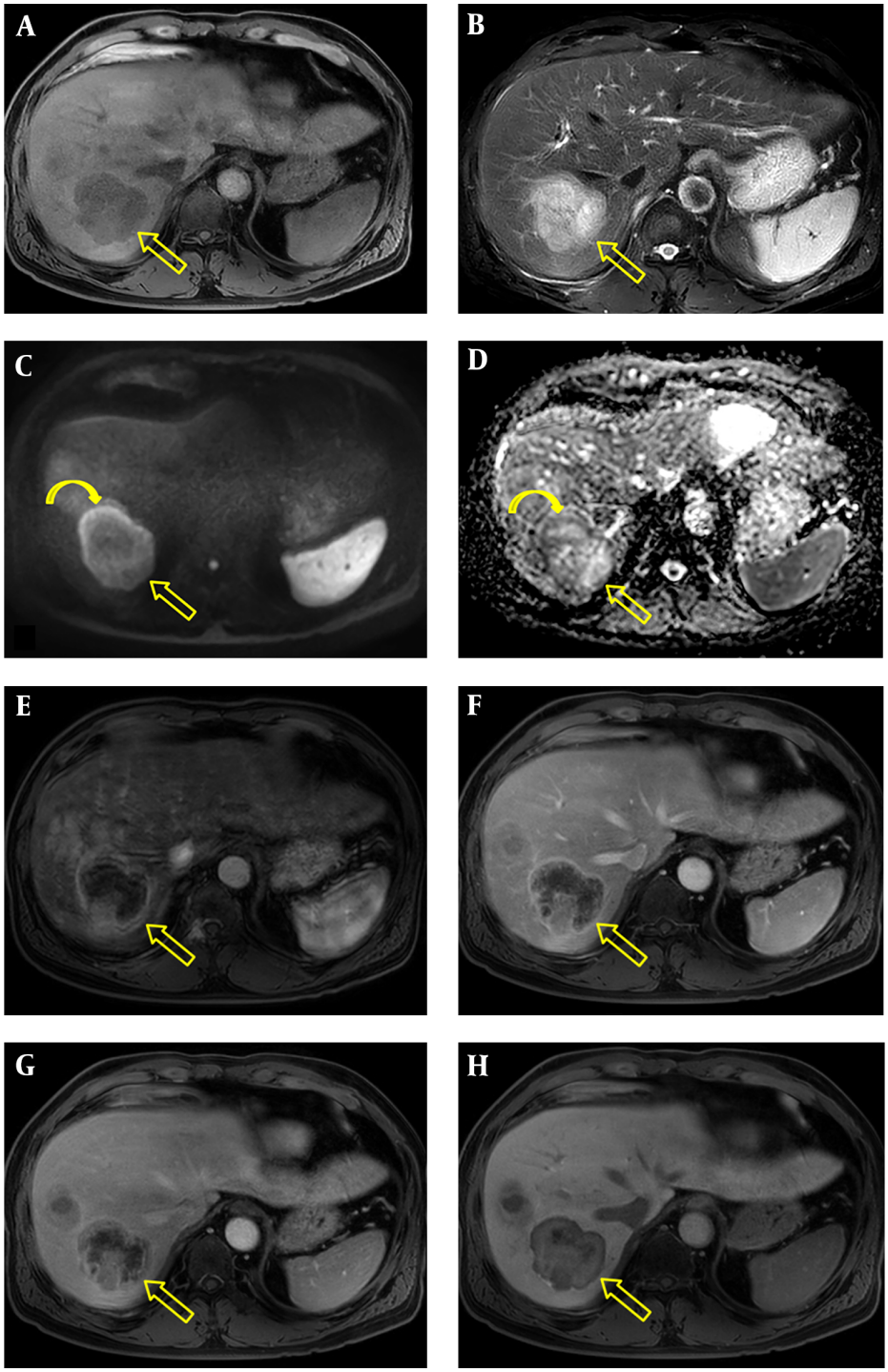

Figure 3. Gadoxetic acid-enhanced and diffusion-weighted MR imaging of scirrhous HCC. A, Axial T1-weighted image shows a hypointense mass with lobulated contours in segment 7 (open arrow); B, Axial T2-weighted image shows a hyperintense mass (open arrow); C and D, Axial diffusion weighted image (b = 800 s/mm^2) and apparent diffusion coefficient map show diffusion restriction (curved arrows) in the periphery of the mass (open arrows); E - G, Axial contrast-enhanced arterial, portal venous, and 2-minute delayed phase images show arterial rim-like enhancement and subsequent centripetal enhancement of the mass (open arrows); H, The mass (open arrow) has a target appearance consisting of central enhancement and a thin peripheral hypointense rim on hepatobiliary phase image.

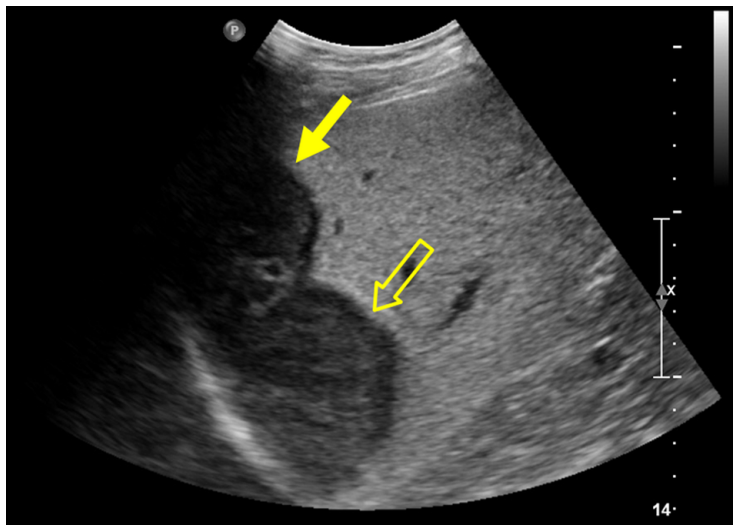

Figure 4. Ultrasonography image shows two hypoechoic hepatic masses (arrow and open arrow) with abutment in the right hepatic lobe.

were scirrhous type (3). Scirrhous HCCs have unique histologic features characterized by abundant fibrous stroma admixed with tumor cells, and unusual capsule, hemorrhage, and necrosis (3, 10). In our case, the scirrhous type HCC had intense fibrosis and no tumor capsule or necrosis, which was similar to results of previous studies (3, 10), whereas the classic HCC showed a partial capsule. Clinically, scirrhous HCC usually develops in patients with chronic liver disease and occasionally releases parathyroid hormone-related protein, resulting in hypercalcemia and hypophosphatemia (3, 4, 9, 11). Our subject had early cirrhotic liver but showed normal levels of calcium and phosphate.

The classic and scirrhous HCCs in our subject showed definite differences in imaging features on gadoxetic acid-enhanced and DW MR imaging. The classic HCC in segment 8 showed arterial hyperenhancement, washout, capsule, and hemorrhage, which were consistent with a diagnosis of HCC according to the American association for the study of liver disease guideline and liver imaging-reporting and data system (12). In contrast, the scirrhous HCC in segment 7 revealed peripheral rim enhancement on arterial phase, followed by centripetal enhancement on portal venous and delayed phases, and peripheral diffusion restriction. On HBP image the scirrhous HCC showed a target appearance of central enhancement with peripheral hypointensity. These imaging findings of scirrhous type HCC were consistent with characteristic histopathologic features of central fibrosis and peripheral tumor cellular tissue. Yoshikawa et al. (13) reported that histologically fibrous tissue showed delayed enhancement on CT, and Kim et al. (4) demonstrated that the common enhancement pattern of scirrhous HCC was peripheral rim-like enhancement on the arterial and portal venous phases followed by central enhancement on the equilibrium phase on dynamic enhanced CT. A previous study (7) described that a target appearance on HBP and DW image was a common feature of scirrhous HCC on gadoxetic acid-enhanced and DW MR imaging. However, these imaging findings are also commonly observed in other malignant liver tumors containing fibrosis such as IHCC, fibrolamellar HCC, and metastases (7, 8, 14). Although Park et al. (7) reported that arterial hyperenhancement representing 20% or more of the tumor diameter is a helpful MR imaging finding for discrimination of scirrhous HCC from IHCC, it is difficult to differentiate scirrhous HCC from other hepatic tumors with fibrosis based on imaging features in daily practice because of its low incidence and overlapping imaging findings with other tumor types (4, 15).

Some studies reported that primary hepatic cancers such as combined hepatocellular and cholangiocarcinomas (combined HCC-CC) and certain HCCs arose from hepatic progenitor cells and showed dual (hepatocellular/biliary) phenotypes (16, 17). Park et al. (15) described that scirrhous HCC is characterized by an intermediate pattern between HCC and cholangiocarcinoma in pathologic findings and might develop from hepatic progenitor cells. Some investigators demonstrated that primary hepatic neoplasm of intermediate phenotype showed an aggressive clinical course (18, 19); however, Kim et al. (4) reported that overall survival after surgery of patients with scirrhous HCC does not differ from that of patients with classic HCC. In our case, there was no evidence of lymph node metastasis in surgery and no recurrence until the 16-

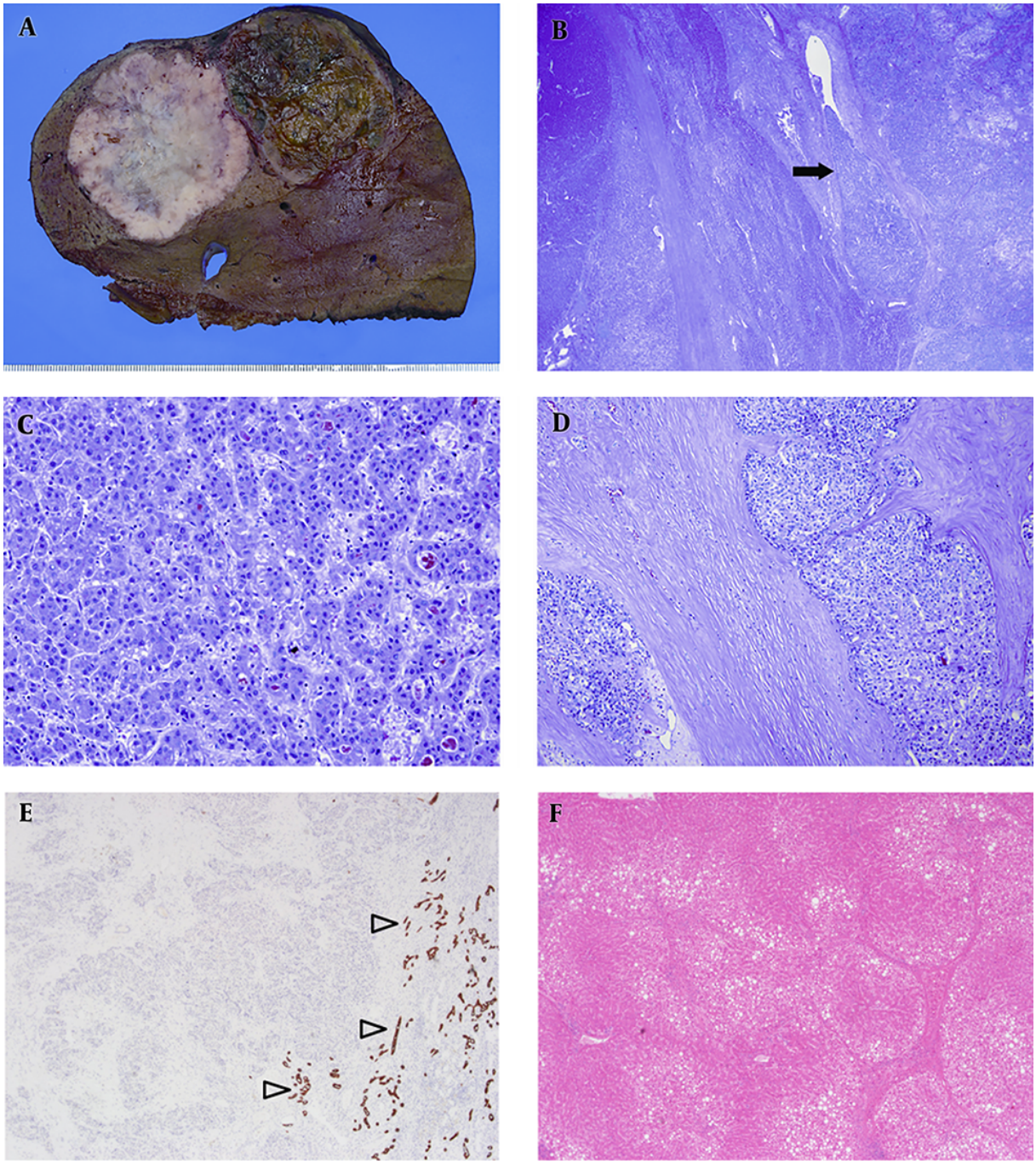

Figure 5. A, Resected liver demonstrates two masses: the mass in segment 8 is a large nodule with brownish cut surface and foci of hemorrhage, while the mass in segment 7 is characterized by lobulated contour and whitish cut surface; B, In low-power view, the two tumors were distinctly separated by non-neoplastic liver and vascular invasion (arrow) was also noted; C, The tumor in segment 8 shows polygonal tumor cells with eosinophilic cytoplasm that are distributed in a trabecular and pseuoglandular pattern; D, The tumor in segment 7 shows nests of polygonal round cells embedded within abundant fibrous stroma; E, Cytokeratin (CK) 19 immunostaining highlights normal bile ducts (open arrowheads). However, the tumors in segment 7 and 8 are negative for CK19 immunostaining; F, Complete and vague nodular change of the liver with moderate fatty change was found that is consistent with early cirrhosis.

month follow-up. Scirrhous HCC is thought to be a unique neoplasm phenotypically between HCC and cholangiocarcinoma.

Even though percutaneous liver biopsy was performed, scirrhous HCC was misdiagnosed as IHCC prior to surgery. Omata et al. (9) reported that there was no correctly diagnosed case from premortem biopsies for 16 scirrhous HCCs, and most were misdiagnosed as metastatic adenocarcinomas. Kim et al. (8) similarly demonstrated that two of three scirrhous HCCs were histopathologically mistaken for poorly differentiated adenocarcinoma and combined HCC-CC before surgery. Percutaneous biopsy yields only a fraction of the tumor tissue and scirrhous HCC has abundant fibrous stroma, therefore it is prone to be misidentified as adenocarcinoma. In particular, when poorly differentiated cells are obtained, as in our case, it is difficult to know the origin of the cells even when immunohistochemical staining is performed. These problems make it difficult to diagnose scirrhous HCC through percutaneous biopsy.

In summary, we report synchronous occurrence of classic and scirrhous HCCs in a patient with early liver cirrhosis. Scirrhous HCC shows different imaging findings from classic HCC due to its histopathological characteristics and is easily misdiagnosed as other hepatic tumors containing fibrosis, such as IHCC. Despite its rarity, radiologists should be aware of scirrhous HCC as one of the malignant hepatic neoplasms with abundant fibrosis.

Footnotes

Authors' Contributions: None declared.

Conflict of Interests: The authors declare that they have no conflict of interest.

Financial Disclosure: None declared.

Funding/Support: This work was supported by the Soonchunhyang University Research Fund.

References

1. Bruix J, Sherman M, Practice Guidelines Committee AAFTSOLD. Management of hepatocellular carcinoma. *Hepatology*. 2005;**42**(5):1208–36. doi: 10.1002/hep.20933. [PubMed: 16250051].
2. Eggert T, McGlynn KA, Duffy A, Manns MP, Greten TF, Altekruse SF. Fibrolamellar hepatocellular carcinoma in the USA, 2000-2010: A detailed report on frequency, treatment and outcome based on the Surveillance, Epidemiology, and End Results database. *United European Gastroenterol J*. 2013;**1**(5):351–7. doi: 10.1177/2050640613501507. [PubMed: 24917983]. [PubMed Central: PMC4040774].
3. Kurogi M, Nakashima O, Miyaaki H, Fujimoto M, Kojiro M. Clinicopathological study of scirrhous hepatocellular carcinoma. *J Gastroenterol Hepatol*. 2006;**21**(9):1470–7. doi: 10.1111/j.1440-1746.2006.04372.x. [PubMed: 16911695].
4. Kim SH, Lim HK, Lee WJ, Choi D, Park CK. Scirrhous hepatocellular carcinoma: comparison with usual hepatocellular carcinoma based on CT-pathologic features and long-term results after curative resection. *Eur J Radiol*. 2009;**69**(1):123–30. doi: 10.1016/j.ejrad.2007.09.008. [PubMed: 17976942].
5. Yamashita Y, Fan ZM, Yamamoto H, Matsukawa T, Arakawa A, Miyazaki T, et al. Sclerosing hepatocellular carcinoma: radiologic findings. *Abdom Imaging*. 1993;**18**(4):347–51. [PubMed: 8220034].
6. Chen F, Li HJ, Zhao DW, Feng JL, Ding JL. Rare CT and MR imaging features of scirrhous hepatocellular carcinoma with gross specimen and pathologic correlation: Case report and review of the literature. *Radiol Infect Dis*. 2015;**2**(3):137–40. doi: 10.1016/j.jrid.2015.07.003.
7. Park MJ, Kim YK, Park HJ, Hwang J, Lee WJ. Scirrhous hepatocellular carcinoma on gadoxetic acid-enhanced magnetic resonance imaging and diffusion-weighted imaging: emphasis on the differentiation of intrahepatic cholangiocarcinoma. *J Comput Assist Tomogr*. 2013;**37**(6):872–81. doi: 10.1097/RCT.0b013e31829d44c1. [PubMed: 24270108].
8. Kim SH, Lee WJ, Lim HK, Park CK. Sclerosing hepatic carcinoma: helical CT features. *Abdom Imaging*. 2007;**32**(6):725–9. doi: 10.1007/s00261-006-9174-0. [PubMed: 17203330].
9. Omata M, Peters RL, Tatter D. Sclerosing hepatic carcinoma: relationship to hypercalcemia. *Liver*. 1981;**1**(1):33–49. [PubMed: 6294435].
10. Iha H. Clinicopathological study on scirrhous hepatocellular carcinoma. A study of 12 resected cases. *Kanzo*. 1994;**35**(12):855–63. doi: 10.2957/kanzo.35.855.
11. Albar JP, De Miguel F, Esbrit P, Miranda R, Fernandez-Flores A, Sarasa JL. Immunohistochemical detection of parathyroid hormone-related protein in a rare variant of hepatic neoplasm (sclerosing hepatic carcinoma). *Human Pathol*. 1996;**27**(7):728–31. doi: 10.1016/s0046-8177(96)90405-0.
12. Choi JY, Lee JM, Sirlin CB. CT and MR imaging diagnosis and staging of hepatocellular carcinoma: part II. Extracellular agents, hepatobiliary agents, and ancillary imaging features. *Radiology*. 2014;**273**(1):30–50. doi: 10.1148/radiol.14132362. [PubMed: 25247563]. [PubMed Central: PMC4263770].
13. Yoshikawa J, Matsui O, Kadoya M, Gabata T, Arai K, Takashima T. Delayed enhancement of fibrotic areas in hepatic masses: CT-pathologic correlation. *J Comput Assist Tomogr*. 1992;**16**(2):206–11. [PubMed: 1312098].
14. Chong YS, Kim YK, Lee MW, Kim SH, Lee WJ, Rhim HC, et al. Differentiating mass-forming intrahepatic cholangiocarcinoma from atypical hepatocellular carcinoma using gadoxetic acid-enhanced MRI. *Clin Radiol*. 2012;**67**(8):766–73. doi: 10.1016/j.crad.2012.01.004. [PubMed: 22425613].
15. Park CI, Park YN. Immunohistochemical profile of sclerosing hepatic carcinoma. *Korea J Pathol*. 1994;**28**(6):636–42.
16. Kim H, Park C, Han KH, Choi J, Kim YB, Kim JK, et al. Primary liver carcinoma of intermediate (hepatocyte-cholangiocyte) phenotype. *J Hepatol*. 2004;**40**(2):298–304. [PubMed: 14739102].
17. Maeda A, Ebata T, Matsunaga K, Kanemoto H, Bando E, Yamaguchi S, et al. Primary liver cancer with bidirectional differentiation into hepatocytes and biliary epithelium. *J Hepatobiliary Pancreat Surg*. 2005;**12**(6):484–7. doi: 10.1007/s00534-005-1010-3. [PubMed: 16365824].
18. Wu PC, Fang JW, Lau VK, Lai CL, Lo CK, Lau JY. Classification of hepatocellular carcinoma according to hepatocellular and biliary differentiation markers. Clinical and biological implications. *Am J Pathol*. 1996;**149**(4):1167–75. [PubMed: 8863666]. [PubMed Central: PMC1865193].
19. Robrechts C, De Vos R, Van den Heuvel M, Van Cutsem E, Van Damme B, Desmet V, et al. Primary liver tumour of intermediate (hepatocyte-bile duct cell) phenotype: a progenitor cell tumour? *Liver*. 1998;**18**(4):288–93. [PubMed: 9766827].